Riemannian Level-set methods for Tensor-Valued Data

Mourad Zéraï & Maher Moakher
Laboratory for Mathematical and Numerical Modeling in Engineering Science
National Engineering School at Tunis
ENIT-LAMSIN, B.P. 37, 1002 Tunis Belvédère, Tunisia
mourad.zerai@gmail.com, maher.moakher@enit.rnu.tn

February 11, 2013

Abstract

We present a novel approach for the derivation of PDEs modeling curvature-driven flows for matrix-valued data. This approach is based on the Riemannian geometry of the manifold of Symmetric Positive Definite Matrices $\mathcal{P}(n)$. The differential geometric attributes of $\mathcal{P}(n)$ −such as the bi-invariant metric, the covariant derivative and the Christoffel symbols− allow us to extend scalar-valued mean curvature and snakes methods to the tensor data setting. Since the data live on $\mathcal{P}(n)$, these methods have the natural property of preserving positive definiteness of the initial data. Experiments on three-dimensional real DT-MRI data show that the proposed methods are highly robust.

1 Introduction

With the introduction of diffusion tensor magnetic resonance imaging (DT-MRI) [4], there has been an ever increasing demand on rigorous, reliable and robust methods for the processing of tensor-valued data such as the estimation, filtering, regularization and segmentation. Many well established PDE-based methods used for the processing of scalar-valued data have been extended in various ways to the processing of multi-valued data such as vector-valued data and smoothly constrained data [5, 11, 20, 21, 22, 23]. Recently, some efforts have been directed toward the extension of these methods to tensor fields [3, 8, 7, 13, 16, 24, 25]. The generalization of the methods used for scalar- and vector-valued data to tensor-valued data is being pursued with mainly three formalisms: the use of geometric invariants of tensors like eigenvalues, determinant, trace; the generalization of Di Zenzo's concept of a structure tensor for vector-valued images to tensor-valued data; and recently, differential-geometric methods.

The aim of the present paper is to generalize the total variation (TV) flow, mean curvature motion (MCM), modified mean curvature flow and self snakes to tensor-valued data such as DT-MRI. The key ingredient for these generalizations is the use of the

Riemannian geometry of the space of symmetric positive-definite (SPD) matrices. The remainder of this paper is organized as follows. In Section 2 we give a compilation of results that gives the differential geometry of the Riemannian manifold of symmetric positive-definite matrices. In Section 3 we fix notation and recall some facts about immersions between Riemannian manifolds and their mean curvature. We explain in Section 4 how to describe a DT-MR image by differential-geometric concepts. Section 5 is the key of our paper in which we extend several mean curvature-based flows for the denoising and segmentation from the scalar and vector setting to the tensor one. In Section 6 we present some numerical results.

2 Differential Geometry of $\mathcal{P}(n)$

Positive-definite matrices are omnipresent in many engineering and physical contexts. They play important roles in various disciplines such as control theory, continuum mechanics, numerical analysis, covariance analysis, signal processing, etc. Recently, they gained an increasing attention within the diffusion tensor magnetic resonance imaging (DT-MRI) community as they are used as an encoding for the principal diffusion directions ans strengths in biological tissues.

We here recall some differential-geometric facts about the space of symmetric positive-definite matrices that have been recently published by the authors. We denote by $\mathcal{S}(n)$ the vector space of $n \times n$ symmetric matrices. A matrix $A \in \mathcal{S}(n)$ is said to be positive semidefinite if $\boldsymbol{x}^T A \boldsymbol{x} \geq 0$ for all $\boldsymbol{x} \in \mathbb{R}^n$, and positive definite if in addition A is invertible. The space of all $n \times n$ symmetric, positive-definite matrices will be denoted by $\mathcal{P}(n)$. We note that the set of positive-semidefinite matrices is a pointed convex cone in the linear space of $n \times n$ matrices, and that $\mathcal{P}(n)$ is the interior of this cone. It is a differentiable manifold endowed with a Riemannian structure. The tangent space to $\mathcal{P}(n)$ at any of its points P is the space $T_P\mathcal{P}(n) = \{P\} \times \mathcal{S}(n)$, which for simplicity is identified with $\mathcal{S}(n)$. On each tangent space $T_P\mathcal{P}(n)$ we introduce the base point-dependent inner product defined by $\langle A, B\rangle_P := \operatorname{tr}(P^{-1}AP^{-1}B)$.

This inner product leads to a natural Riemannian metric on the manifold $\mathcal{P}(n)$ that is given at each P by the differential

$$ds^2 = \operatorname{tr}\left(P^{-1}dPP^{-1}dP\right), \tag{1}$$

where dP is the symmetric matrix with elements (dP_{ij}). We note that the metric (1) is invariant under congruent transformations: $P \to LPL^T$ and under inversion $P \to P^{-1}$.

For an $n \times n$ matrix A we denote by $\operatorname{vec} A$ the n^2-column vector that is obtained by stacking the columns of A. If A is symmetric, then then $\frac{1}{2}n(n-1)$ elements of $\operatorname{vec}(A)$ are redundant. We will denote by $\upsilon(A)$ the $d = \frac{1}{2}n(n+1)$-vector that is obtained from $\operatorname{vec}(A)$ by eliminating the redundant elements, e.g., all supradiagonal elements of A. We note that there are several ways to arrange the independent elements of $\operatorname{vec}(A)$ into $\upsilon(A)$. In any case, there exists a unique $n^2 \times \frac{1}{2}n(n+1)$ matrix, called the duplication matrix and denoted by D_n, that by duplicating certain elements, reconstructs $\operatorname{vec} A$ from $\upsilon(A)$, i.e., is the matrix such that

$$\operatorname{vec} A = D_n \upsilon(A). \tag{2}$$

The duplication matrix D_n, which has been studied extensively by Henderson and Searle [9], and by Magnus and Neudecker [14], has full column rank $\frac{1}{2}n(n+1)$. Hence, $D_n^T D_n$ is non-singular and it follows that the duplication matrix D_n has a Moore-Penrose inverse denoted by D_n^+ and is given by

$$D_n^+ = \left(D_n^T D_n\right)^{-1} D_n^T.$$

It follows from (2) that

$$\upsilon(A) = D_n^+ \operatorname{vec} A. \tag{3}$$

By using the vector $\upsilon(P)$ as a parametrization of $P \in \mathcal{P}(n)$ we obtain the matrix of components of the metric tensor associated with the Riemannian metric (1) is given explicitly by [25]

$$G(P) = D_n^T(P^{-1} \otimes P^{-1})D_n. \tag{4}$$

For differential-geometric operators on $\mathcal{P}(n)$ it is important to obtain the expression of the inverse of the metric and that of its determinant. The matrix of components of the inverse metric tensor is given by

$$G^{-1}(P) = D_n^+ \left(P \otimes P\right) {D_n^+}^T, \tag{5}$$

and the determinant of G is

$$\det(G(P)) = 2^{n(n-1)/2} \left((\det(P)\right)^{(n+1)}. \tag{6}$$

In the coordinate system (p^α), the Christoffel symbols are given by [25]

$$\Gamma^\gamma_{\alpha\beta} = -[D_n^T \left(P^{-1} \otimes E^\gamma\right) D_n]_{\alpha\beta}, \quad 1 \le \alpha, \beta, \gamma \le d,$$

where E^γ is the dual basis associated with the local coordinates (p^α). As the elements of E^γ and D_n are either 0, 1, or $\frac{1}{2}$, it follows from the above theorem that each non-vanishing Christoffel symbol is given by an element of P^{-1} or half of it.

Let P be an element of $\mathcal{P}(3)$ and let dP be a (symmetric) infinitesimal variation of it

$$P = \begin{bmatrix} p^1 & p^4 & p^6 \\ p^4 & p^2 & p^5 \\ p^6 & p^5 & p^3 \end{bmatrix}, \qquad dP = \begin{bmatrix} dp^1 & dp^4 & dp^6 \\ dp^4 & dp^2 & dp^5 \\ dp^6 & dp^5 & dp^3 \end{bmatrix}.$$

Hence, the complete and reduced vector forms of P are respectively,

$$\operatorname{vec}(P) = [p^1\ p^4\ p^6\ p^4\ p^2\ p^5\ p^6\ p^5\ p^3]^T, \quad \upsilon(P) = [p^1\ p^2\ p^3\ p^4\ p^5\ p^6]^T.$$

The components of the inverse metric tensor and the Christoffel symbols are given explicitly in the appendix.

3 Immersions and Mean Curvature

Let (M, γ) and (N, g) be two connected Riemanian manifolds of dimensions m and n, respectively. We consider a map $\phi : M \to N$ that is of class C^2, i.e., $\phi \in C^2(M, N)$. Let $\{x^\alpha\} - 1 \leq \alpha \leq m$ be a local coordinate system of x in a neighborhood of a point $p \in M$ and let $\{y^i\}_{1 \leq i \leq n}$ be a local coordinate system of y in a neighborhood of $\phi(P) \in N$.

The mapping ϕ induces a metric $\phi^* g$ on M defined by

$$\phi^* g\left(X_p, Y_p\right) = g\left(\phi_*(X_p), \phi_*(Y_p)\right). \tag{7}$$

This metric is called the *pull-back* metric induced by ϕ, as it maps the metric in the opposite direction of the mapping ϕ.

An isometry is a diffeomorphism $\phi : M \to N$ that preserves the Riemannian metric, i.e., if g and γ are the metrics for M and N, respectively, then $\gamma = \phi^* g$. It follows that an isometry preserves the length of curves, i.e., if c is a smooth curve on M, then the curve $\phi \circ c$ is a curve of the same length on N. Also, the image of a geodesic under an isometry is again a geodesic.

A mapping $\phi : M \to N$ is called an *immersion* if $\left(\phi_*\right)_p$ is injective for every point p in M. We say that M is immersed in N by ϕ or that M is an immersed submanifold of N. When an immersion ϕ is injective, it is called an *embedding* of M into N. We then say that M is an *embedded submanifold*, or simply, a *submanifold* of N.

Now let $\phi : M \to N$ be an immersion of a manifold M into a Riemannian manifold N with metric g. The first fundamental form associated with the immersion ϕ is $h = \phi^* g$. Its components are $h_{\alpha\beta} = \partial_\alpha \phi^i \partial_\beta \phi^j g_{ij}$ where $\partial_\alpha \phi^i = \frac{\partial \phi^i}{\partial x^\alpha}$. The total covariant derivative $\nabla d\phi$ is called the second fundamental form of ϕ and is denoted by $II^M(\phi)$. The second fundamental form II^M takes values in the normal bundle of M. The mean curvature vector $\boldsymbol{H}$ of an isometric immersion $\phi : M \to N$ is defined as the trace of the second fundamental form $II^M(\phi)$ divided by $m = \dim M$ [10]

$$\boldsymbol{H} := \frac{1}{m} \operatorname{tr}_\gamma II^M(\phi). \tag{8}$$

In local coordinates, we have [10]

$$mH^i = \Delta_M \phi^i + \gamma^{\alpha\beta}(x) {}^N\Gamma^i_{jk}\left(\phi(x)\right) \frac{\partial \phi^j}{\partial x^\alpha} \frac{\partial \phi^k}{\partial x^\beta}. \tag{9}$$

where ${}^N\Gamma^i_{jk}$ are the Christoffel symbols of (N, g) and Δ_M is the Laplace-Beltrami operator on (M, γ) given by

$$\Delta_M = \frac{1}{\sqrt{\det \gamma}} \frac{\partial}{\partial x^\alpha} \left(\sqrt{\det \gamma} \gamma^{\alpha\beta} \frac{\partial}{\partial x^\beta} \right). \tag{10}$$

4 Diffusion-Tensor MRI Data as Isometric Immersions

A volumetric tensor-valued image can be described mathematically as an isometric immersion $(x^1, x^2, x^3) \mapsto \phi = (x^1, x^2, x^3; P(x^1, x^2, x^3))$ of a three-dimensional domain Ω in the fiber bundle $\mathbb{R}^3 \otimes \mathcal{P}(3)$, which is a nine-dimensional manifold. We denote by (M, γ) the image manifold and its metric and by (N, g) the target manifold and its metric. Here $M = \Omega$ and $N = \diagdown^3 \otimes \mathcal{P}(3)$. Consequently, a tensor-valued image is a section of this fiber bundle. The metric $\hat{g}$ of N is given by

$$d\hat{s}^2 = ds^2_{\text{spatial}} + ds^2_{\text{tensor}}. \tag{11}$$

The target manifold N, in this context is also called the *space-feature manifold* [23]. We can rewrite the metric defined by (11) as the quadratic form

$$d\hat{s}^2 = (dx^1)^2 + (dx^2)^2 + (dx^3)^2 + (d\boldsymbol{p})^T D_n^T (P^{-1} \otimes P^{-1}) D_n (d\boldsymbol{p}),$$

where $\boldsymbol{p} = (p^i) = \upsilon(P)$. The corresponding metric tensor is

$$\hat{g} = \begin{pmatrix} I_3 & 0_{3,6} \\ 0_{6,3} & g \end{pmatrix},$$

where g is the metric tensor of $\mathcal{P}(3)$ as defined in Section 2.

Since the image is an isometric immersion, we have $\gamma = \phi^* \hat{g}$. Therefore

$$\gamma_{\alpha\beta} = \delta_{\alpha\beta} + g_{ij} \partial_\alpha p^i \partial_\beta p^j, \quad \alpha, \beta = 1, \ldots, m, \quad i, j = 1, \ldots, d. \tag{12}$$

We note that $d = n - m$ is the codimension of M. In compact form, we have

$$\gamma = I_m + (\nabla \boldsymbol{p})^T G(\phi) \nabla \boldsymbol{p}. \tag{13}$$

where G is given by (4). (We take $m = 2$ for a slice and $m = 3$ for a volumetric DT-MRI image.)

5 Geometric Curvature-Driven Flows for Tensor-Valued Data

The basic concept in which geometric curvature-driven flows are based is the mean curvature of a submanifold embedded in a higher dimensional manifold. Here we generalize the scalar mean curvature flow to mean curvature flow in the space-feature manifold $\Omega \otimes \mathcal{P}(3)$. For this, we embed the Euclidean image space Ω into the Riemannian manifold $\Omega \otimes \mathcal{P}(3)$, and use some classical results from differential geometry to derive the *Riemannan Mean Curvature* (RMC). We then use the RMC to generalize mean curvature flow to the tensor-valued data. Given the expression of the mean curvature vector $\boldsymbol{H}$, we can establish some PDEs based tensor-image filtering. Especially, we are interested of the so called level-set methods, which relay on PDEs that modify the shape of level sets in an image.

5.1 Riemannian Total Variation Flow

The total variation norm (TV) method introduced in [19] and its reconstructions have been successfully used in reducing noise and blurs without smearing sharp edges in grey-level, color and other vector-valued images [6, 12, 17, 20, 21, 22]. It is then natural to look for the extension of the TV norm to tensor-valued images.

The TV norm method is obtained as a gradient-decent flow associated with the L^1-norm of the tensor field. This yields the following PDE that express the motion by the mean curvature vector $\boldsymbol{H}$

$$\partial_t \phi^i = H^i. \tag{14}$$

This flow can be considered as a deformation of the tensor field toward *minimal immersion*. Indeed, it derives from variational setting that minimize the *volume* of the embedded image manifold in the space-feature manifold.

5.2 Riemannian Mean Curvature Flow

The following flow was proposed for the processing of scalar-valued images

$$\partial_t u = |\nabla u| \operatorname{div} \frac{\nabla u}{|\nabla u|}, \quad u(0,x,y) = u_0(x,y), \tag{15}$$

where $u_0(x,y)$ is the grey level of the image to be processed, $u(t,x,y)$ is its smoothed version that depends on the scale parameter t.

The "philosophy" of this flow is that the term $|\nabla u| \operatorname{div} \frac{\nabla u}{|\nabla u|}$ represents a degenerate diffusion term which diffuses u in the direction orthogonal to its gradient ∇u and does not diffuse at all in the direction of ∇u.

This formulation has been proposed as a "morphological scale space" [2] and as more numerically tractable method of solving total variation [15].

The natural generalization of this flow to tensor-valued data is

$$\partial_t \phi^i = |\nabla^\gamma \phi|_g H^i, \quad i = 1, \ldots, d. \tag{16}$$

where

$$|\nabla^\gamma \phi|_g = \gamma^{\alpha\beta} g_{ij} \partial_\alpha \phi^i \partial_\beta \phi^j.$$

We note that several authors have tried to generalize curvature-driven flows for tensor-valued data in different ways. We think that the the use of differential-geometric tools and concepts yield the correct generalization.

5.3 Modified Riemannian Mean Curvature Flow

To denoise highly degraded images, Alvarez et al. [1] have proposed a modification of the mean curvature flow equation (15) that reads

$$\partial_t \phi = c\left(|K \star \nabla \phi|\right) |\nabla \phi| \operatorname{div} \frac{\nabla \phi}{|\nabla \phi|}, \quad \phi(0,x,y) = \phi_0(x,y), \tag{17}$$

where K is a smoothing kernel (a Gaussian for example), $K \star \nabla \phi$ is therefore a local estimate of $\nabla \phi$ for noise elimination, and $c(s)$ is a nonincreasing real function which tends to zero as $s \to \infty$. We note that for the numerical experiments we have used $c(|\nabla \phi|) = k^2/(k^2 + |\nabla \phi|^2)$.

The generalization of the modified mean curvature flow to tensor-field processing is

$$\partial_t \phi^i = c\left(|K \star \nabla^\gamma \phi|_g\right) |\nabla^\gamma \phi|_g H^i, \quad \phi^i(0,\Omega) = \phi^i_0(\Omega), \tag{18}$$

The role of c is to reduce the magnitude of smoothing near edges. In the scalar case, this equation does not have the same action as the Perona-Malik equation of enhancing edges. Indeed, Perona-Malik equation has variable diffusivity function and has been shown to selectively produce a "negative diffusion" which can increase the contrast of edges. Equation of he form (17) have always positive or forward diffusion, and the term c merely reduces the magnitude of that smoothing. To correct this situation, Sapiro have proposed the self-snakes formalism [20], which we present in the next subsection and generalize to the matrix-valued data setting.

5.4 Riemannan Self-Snakes

The method of Sapiro, which he names *self-snakes* introduces an edge-stopping function into mean curvature flow

$$\begin{aligned} \partial_t \phi &= |\nabla \phi| \operatorname{div}\left(c\left(K \star |\nabla \phi|\right) \tfrac{\nabla \phi}{|\nabla \phi|}\right) \\ &= c\left(K \star |\nabla \phi|\right) |\nabla \phi| \operatorname{div}\left(\tfrac{\nabla \phi}{|\nabla \phi|}\right) + \nabla c\left(K \star |\nabla \phi|\right) \cdot \nabla \phi \end{aligned} \tag{19}$$

Comparing equation (19) to (17), we observe that the term $\nabla c\left(K \star |\nabla \phi|\right) \cdot \nabla \phi$ is missing in the old model. This is due to the fact that the Sapiro model takes into account the image structure. Indeed, equation (19) can be re-written as

$$\partial_t \phi = \mathcal{F}_{\text{diffusion}} + \mathcal{F}_{\text{shock}}, \tag{20}$$

where

$$\mathcal{F}_{\text{diffusion}} = c\left(K \star |\nabla \phi|\right) |\nabla \phi| \operatorname{div}\left(\frac{\nabla \phi}{|\nabla \phi|}\right),$$

$$\mathcal{F}_{\text{shock}} = \nabla c\left(K \star |\nabla \phi|\right) \cdot \nabla \phi.$$

The term $\mathcal{F}_{\text{diffusion}}$ is as in the anisotropic flow proposed in [1]. The second term in (20), i.e., $\nabla c \cdot \nabla \phi$, increases the attraction of the deforming contour toward the boundary of "objects" acting as the shock-filter introduced in [18] for deblurring. Therefore, the flow $\nabla c \cdot \nabla \phi$ is a shock filter acting like the backward diffusion in the Perona-Malik equation, which is responsible for the edge-enhancing properties of self snakes. See [20] for detailed discussion on this topic.

We are now interested in generalizing Self-Snakes method for the case of tensor-valued data. We will start the generalization from equation (20) in the following manner

$$\partial_t \phi = \mathcal{F}_{\mathit{diffusion}} + \mathcal{F}_{\mathit{shock}}, \tag{21}$$

where

$$\begin{aligned} \mathcal{F}_{\mathit{diffusion}} &= c\left(K \star |\nabla^\gamma \phi|_g\right) |\nabla^\gamma \phi|_g H^i \\ \mathcal{F}_{\mathit{shock}} &= \nabla c\left(K \star |\nabla^\gamma \phi|_g\right) \cdot \nabla^\gamma \phi^i. \end{aligned} \tag{22}$$

This decomposition is not artificial, since the covariant derivative on follow the same chain rule as the Euclidean directional derivative: let V a vector field on M which components are v^i, and let ρ a scalar function. From the classic differential geometry we have

$$\nabla_i^\gamma(\rho v^i) = \rho \nabla_i^\gamma v^i + v^i \nabla_i^\gamma \rho \tag{23}$$

and in compact form

$$\mathrm{div}_\gamma(\rho V) = \rho \, \mathrm{div}_\gamma \, V + V \cdot \mathrm{grad}_\gamma \rho. \tag{24}$$

6 Numerical Experiments

In Fig. 1 (left), we give a slice of a 3D tensor field defined over a square in $\mathbb{R}^2$. We note that a symmetric positive-definite 3×3 matrix P is represented graphically by an ellipsoid whose principal directions are parallel to the eigenvectors of P and whose axes are proportional to the eigenvalues of P^{-1}. Figure 1 (right) shows this tensor field after the addition of noise. The resultant tensor field $P_0(x^1, x^2, x^3)$ is used as an initial condition for the partial differential equations (21) which we solve by a finite difference scheme with Neumann boundary conditions. We used 50 time steps of 0.01.s. Figure 2 represents the tensor smoothed by (21).

Figure 1: Original tensor field (left)and noisy tensor field (right).

In this paper we generalized several curvature-driven flows of scalar- and vector-valued data to tensor-valued data. The use of the differential-geometric tools and concepts yields a natural extension of these well-known scalar-valued data processing methods to tensor-valued data processing.

References

[1] L. ALVAREZ, P-L. LIONS AND J-M. MOREL, *Image selective smoothing and edge detection by nonlinear diffusion (II)*, SIAM J. Num. Anal., **29** (1992), pp. 845–866.

[2] L. ALVAREZ AND J-M. MOREL, *A Morphological Approach to Multiscale Analysis: From Principles to Equations*, Kluwler Academic Publishers, 1994.

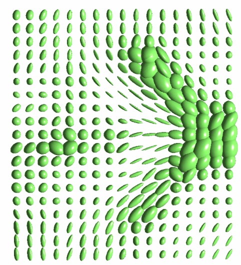

Figure 2: Tensor field smoothed by the Riemannian self snake flow.

[3] V. Arsigny, P. Fillard, X. Pennec, and N.Ayache, *Fast and simple calculus on tensors in the Log-Euclidean framework*, in Proc. 8th Int. Conf. on Medical Image Computing and Computer-Assisted Intervention - MICCAI 2005, Part I, J. Duncan and G. Gerig, eds., vol. 3749 of LNCS, Palm Springs, CA, 2005, Springer Verlag, pp. 115–122.

[4] P. J. Basser, J. Matiello, and D. LeBihan, *MR diffusion tensor spectroscopy and imaging*, Biophysical J., **66** (1994), pp. 259–267.

[5] P.V. Blomgren and T.F. Chan,*Color TV: Total variation methods for restoration of vector valued images*, IEEE Trans. Image Processing, **7** (1998), pp. 304–378.

[6] A. Cumani, *Edge detection in multiscale images*, CVGIP: Graphical Models and Image Processing, **53** (1991), pp. 40–51.

[7] R. Deriche, D. Tschumperlé, C. Lenglet, and M. Rousson, *Variational approaches to the estimation, regularization and segmentation of diffusion tensor Images*, in Mathematical Models in Computer Vision: The Handbook, N. Paragios, Y. Chen and O. Faugeras, eds., Springer, 2005.

[8] C. Feddern, J. Weickert, B. Burgeth, and M. Welk, *Curvature-driven PDE methods for matrix-valued images*, Int. J. Comput. Vision, **69** (2006), pp. 93–107.

[9] H. V. Henderson and S. R. Searle, *Vec and vech operators for matrices, with some uses in Jacobians and multivariate statistics*, Canad. J. Statist., **7** (1979), pp. 65–81.

[10] J. Jost, Riemannian Geometry and Geometric Analysis, Springer, Berlin, 2nd ed., 1998.

[11] R. Kimmel, R. Malladi, and N. Sochen, *Images as embedded maps and minimal surfaces: movies, color, texture, and volumetric medical images*, Int. J. Compt. Vision, **39** (2000), pp. 111–129.

[12] H-C. LEE AND D.R. COK., *Detecting boundaries in a vector field*, IEEE Trans. Signal Proc., **39** (1991), pp. 1181–1194.

[13] C. LENGLET, M. ROUSSON, R. DERICHE, AND O. FAUGERAS, *Statistics on the manifold of multivariate normal distributions: Theory and application to diffusion tensor MRI processing*, J. Mathematical Imaging and Vision, (2006), in Press.

[14] J. R. MAGNUS AND H. NEUDECKER, *The elimination matrix: some lemmas and applications*, SIAM J. Alg. Disc. Meth., **1** (1980), pp. 422–449.

[15] A. MARQUINA AND S. OSHER, *Explicit algoritms for a new time dependent model based on level set motion for non-linear deblurring and noise removal*, SIAM J. Sci. Compt., **22** (2000), pp. 378–405.

[16] M. MOAKHER AND P. G. BATCHELOR, *The symmetric space of positive definite tensors: From geometry to applications and visualization*, in Visualization and Processing of Tensor Fields, J. Weickert and H. Hagen, eds., Berlin, 2005, Springer, pp. 285–298.

[17] R. NEVIATA, *A color edge detector and its use in scene segmentation*, IEEE Trans. Syst. Man. Cybern., **7** (1977), pp. 820–826.

[18] S. OSHER AND L. RUDIN, *Feature-oriented image enhancement using shock filters*, SIAM Journal of Numerical Analysis, **27(4)** (1990), pp. 919–940.

[19] L. RUDIN, S. OSHER, AND E. FATEMI, *Nonlinear Total Variation Based Noise Removal Algorithms*, Physica D, **60** (1992), pp. 259–268.

[20] G. SAPIRO, *Color snakes.*, Technical Report HPL-95-113, Hewlett Packard Computer Peripherals Laboratory, September (1995).

[21] G. SAPIRO, *Vector-valued active contours*, In Proceedings of Computer Vision and Pattern Recognition (CVPR'96), (1996), pp. 520–525.

[22] G. SAPIRO AND D. RINGACH, *Anisotropic diffusion of multivalued images with applications to color filtering*, IEEE Transactions Image Processing., **5** (1996), pp. 1582–1586.

[23] N. A. SOCHEN, R. KIMMEL, AND R. MALLADI, *A general framework for low level vision*, IEEE Trans. Image Process., **7** (1998), pp. 310–318.

[24] J. WEICKERT AND H. HAGEN, eds., Visualization and Processing of Tensor Fields, Springer, Berlin, 2005.

[25] M. ZÉRAÏ AND M. MOAKHER, *The Riemannian geometry of the space of positive-definite matrices and its application to the regularization of diffusion tensor MRI data*, Submitted to: J. Mathematical Imaging and Vision, (2006).

Appendix

We give here the explicit form of the inverse metric tensor and Christoffel symbols for the Riemannian metric on $\mathcal{P}(3)$. The components of the inverse metric tensor are given by

$$G^{-1} = \begin{bmatrix} (p^1)^2 & (p^4)^2 & (p^6)^2 & p^1p^4 & p^4p^6 & p^1p^6 \\ (p^4)^2 & (p^2)^2 & (p^5)^2 & p^2p^4 & p^2p^5 & p^4p^5 \\ (p^6)^2 & (p^5)^2 & (p^3)^2 & p^6p^5 & p^5p^3 & p^6p^3 \\ p^1p^4 & p^2p^4 & p^6p^5 & \frac{1}{2}(p^1p^2+(p^4)^2) & \frac{1}{2}(p^4p^5+p^6p^2) & \frac{1}{2}(p^1p^5+p^4p^6) \\ p^4p^6 & p^2p^5 & p^5p^3 & \frac{1}{2}(p^4p^5+p^6p^2) & \frac{1}{2}((p^5)^2+p^2p^3) & \frac{1}{2}(p^6p^5+p^4p^3) \\ p^1p^6 & p^4p^5 & p^6p^3 & \frac{1}{2}(p^1p^5+p^4p^6) & \frac{1}{2}(p^6p^5+p^4p^3) & \frac{1}{2}(p^1p^3+(p^6)^2) \end{bmatrix}.$$

The determinant of P is $\rho = \det P = p^1p^2p^3+2p^4p^5p^6-p^1(p^5)^2-p^2(p^6)^2-p^3(p^4)^2$,. Let $\boldsymbol{s} := [s^1, s^2, s^3, s^4, s^5, s^6]^T = v(\operatorname{adj}(P))$, where $\operatorname{adj}(P) = \rho P^{-1}$ is the adjoint matrix of P.

The Christoffel symbols are arranged in the following six symmetric matrices:

$$\Gamma^1 = \frac{-1}{\rho}\begin{bmatrix} s^1 & 0 & 0 & s^4 & 0 & s^6 \\ 0 & 0 & 0 & 0 & 0 & 0 \\ 0 & 0 & 0 & 0 & 0 & 0 \\ s^4 & 0 & 0 & s^2 & 0 & s^5 \\ 0 & 0 & 0 & 0 & 0 & 0 \\ s^6 & 0 & 0 & s^5 & 0 & s^3 \end{bmatrix}, \qquad \Gamma^2 = \frac{-1}{\rho}\begin{bmatrix} 0 & 0 & 0 & 0 & 0 & 0 \\ 0 & s^2 & 0 & s^4 & s^5 & 0 \\ 0 & 0 & 0 & 0 & 0 & 0 \\ 0 & s^4 & 0 & s^1 & s^6 & 0 \\ 0 & s^5 & 0 & s^6 & s^3 & 0 \\ 0 & 0 & 0 & 0 & 0 & 0 \end{bmatrix},$$

$$\Gamma^3 = \frac{-1}{\rho}\begin{bmatrix} 0 & 0 & 0 & 0 & 0 & 0 \\ 0 & 0 & 0 & 0 & 0 & 0 \\ 0 & 0 & s^3 & 0 & s^5 & s^6 \\ 0 & 0 & 0 & 0 & 0 & 0 \\ 0 & 0 & s^5 & 0 & s^2 & s^4 \\ 0 & 0 & s^6 & 0 & s^4 & s^1 \end{bmatrix}, \qquad \Gamma^4 = \frac{-1}{2\rho}\begin{bmatrix} 0 & s^4 & 0 & s^1 & s^6 & 0 \\ s^4 & 0 & 0 & s^2 & 0 & s^5 \\ 0 & 0 & 0 & 0 & 0 & 0 \\ s^1 & s^2 & 0 & 2s^4 & s^5 & s^6 \\ s^6 & 0 & 0 & s^5 & 0 & s^3 \\ 0 & s^5 & 0 & s^6 & s^3 & 0 \end{bmatrix},$$

$$\Gamma^5 = \frac{-1}{2\rho}\begin{bmatrix} 0 & 0 & 0 & 0 & 0 & 0 \\ 0 & 0 & s^5 & 0 & s^2 & s^4 \\ 0 & s^5 & 0 & s^6 & s^3 & 0 \\ 0 & 0 & s^6 & 0 & s^4 & s^1 \\ 0 & s^2 & s^3 & s^4 & 2s^5 & s^6 \\ 0 & s^4 & 0 & s^1 & s^6 & 0 \end{bmatrix}, \quad \Gamma^6 = \frac{-1}{2\rho}\begin{bmatrix} 0 & 0 & s^6 & 0 & s^4 & s^1 \\ 0 & 0 & 0 & 0 & 0 & 0 \\ s^6 & 0 & 0 & s^5 & 0 & s^3 \\ 0 & 0 & s^5 & 0 & s^2 & s^4 \\ s^4 & 0 & 0 & s^2 & 0 & s^5 \\ s^1 & 0 & s^3 & s^4 & s^5 & 2s^6 \end{bmatrix}.$$